NASA TECHNICAL NOTE

NASA TN D-6628

NASA TN D-6628
c.1

LOAN COPY: RETUR
AFWL (DOUL)
KIRTLAND AFB, N.

TECH LIBRARY KAFB, NM
0133357

# EFFECT OF REYNOLDS NUMBER ON OVERALL PERFORMANCE OF A 3.7-INCH-DIAMETER SIX-STAGE AXIAL-FLOW COMPRESSOR

*by Laurence J. Heidelberg and Calvin L. Ball*

*Lewis Research Center*
*Cleveland, Ohio 44135*

NATIONAL AERONAUTICS AND SPACE ADMINISTRATION • WASHINGTON, D. C. • FEBRUARY 1972

TECH LIBRARY KAFB, NM
0133357

| 1. Report No. | 2. Government Accession No. | 3. Recipient's Catalog No. |
|---|---|---|
| NASA TN D-6628 | | |

| 4. Title and Subtitle | 5. Report Date |
|---|---|
| EFFECT OF REYNOLDS NUMBER ON OVERALL PERFORMANCE OF A 3.7-INCH-DIAMETER SIX-STAGE AXIAL-FLOW COMPRESSOR | February 1972 |
| | 6. Performing Organization Code |
| 7. Author(s)<br>Laurence J. Heidelberg and Calvin L. Ball | 8. Performing Organization Report No.<br>E-6522 |
| | 10. Work Unit No.<br>764-74 |
| 9. Performing Organization Name and Address<br>Lewis Research Center<br>National Aeronautics and Space Administration<br>Cleveland, Ohio 44135 | 11. Contract or Grant No. |
| | 13. Type of Report and Period Covered<br>Technical Note |
| 12. Sponsoring Agency Name and Address<br>National Aeronautics and Space Administration<br>Washington, D.C. 20546 | 14. Sponsoring Agency Code |

15. Supplementary Notes

16. Abstract

A 9.4-centimeter (3.7-in.) diameter six-stage axial-flow compressor was tested in argon over a range of inlet pressures corresponding to a Reynolds number range of $3.6\times10^4$ to $16.0\times10^4$. The effect of Reynolds number on efficiency, pressure ratio, work input, maximum flow, and surge is shown. The Reynolds number effects are discussed in terms of changes in boundary-layer thickness, losses, and the resulting changes in throughflow velocity. Significant deviation was noted from the 0.2 power relation often used to express the variation of loss with Reynolds number.

| 17. Key Words (Suggested by Author(s)) | 18. Distribution Statement |
|---|---|
| Axial-flow compressor<br>Multistage compressor<br>Reynolds number<br>Brayton cycle | Unclassified - unlimited |

| 19. Security Classif. (of this report) | 20. Security Classif. (of this page) | 21. No. of Pages | 22. Price* |
|---|---|---|---|
| Unclassified | Unclassified | 21 | $3.00 |

* For sale by the National Technical Information Service, Springfield, Virginia 22151

# EFFECT OF REYNOLDS NUMBER ON OVERALL PERFORMANCE OF A 3.7-INCH-DIAMETER SIX-STAGE AXIAL-FLOW COMPRESSOR

by Laurence J. Heidelberg and Calvin L. Ball

Lewis Research Center

## SUMMARY

An experimental investigation was conducted to determine the Reynolds number effect on overall performance in argon for a 9.4-centimeter (3.7-in.) diameter six-stage axial-flow compressor. This compressor is applicable for a 10-kilowatt Brayton cycle space electrical power generation system. The compressor inlet pressure was varied to obtain a range of Reynolds number from $3.6\times10^4$ to $16.0\times10^4$. The effect of inlet pressure and thus Reynolds number on efficiency, pressure ratio, work input, maximum flow, and surge is shown. Efficiency, pressure ratio, weight flow at maximum efficiency, work input, and maximum flow decreased with decreasing Reynolds number. These trends are discussed in terms of increasing boundary-layer thickness, increasing losses, and the resulting increase in throughflow velocity with decreasing Reynolds number. Significant deviation was noted from the 0.2 power relation often used to express the variation of loss with Reynolds number. A comparison of Reynolds number effect for this axial-flow compressor with that of a centrifugal compressor designed for the same overall conditions showed the centrifugal compressor to be less sensitive to Reynolds number.

## INTRODUCTION

The NASA Lewis Research Center is presently engaged in a research program on small centrifugal and axial-flow compressors for application to closed Brayton cycle space electric power generation systems. The program is directed primarily toward establishing the performance level that can be achieved by these machines and to determine the effect of Reynolds number on their performance.

As part of meeting the objectives of this program, a study was conducted on a 15.2-centimeter (6-in.) diameter radial-bladed centrifugal compressor and a six-stage, 9.4-centimeter (3.7-in.) diameter axial-flow compressor. These compressors were designed for a two-shaft 10-kilowatt Brayton cycle space-power system. The overall performance of the centrifugal compressor is reported in reference 1. The effect of Reynolds number on the performance is reported in reference 2. A progressive degradation in performance of the centrifugal compressor resulted as Reynolds number was reduced. The six-stage, 9.4-centimeter (3.7-in.) diameter axial-flow compressor provides a direct comparison with the centrifugal compressor since both compressors were designed for the same overall conditions. The axial-flow compressor design and fabrication is presented in reference 3. The overall performance is reported in reference 4.

This report presents the effect of Reynolds number on the performance of the six-stage compressor. In addition, a comparison with the Reynolds number effect on the 15.2-centimeter (6-in.) diameter centrifugal compressor is made.

Overall argon performance is presented for five inlet pressure levels from 1.4 to 6.2 $N/cm^2$ abs (2.0 to 9.0 psia) at design speed. Data were obtained over a range of weight flows from maximum flow to surge conditions. Performance is presented based on the flow conditions at the compressor inlet and the collector exit. The compressor performance presented herein was obtained at the Lewis Research Center.

## SYMBOLS

| | |
|---|---|
| c | cord length measured at tip of first rotor, m; ft |
| IGV | inlet guide vanes |
| N | compressor rotational speed, rpm |
| $N/\sqrt{\theta}$ | equivalent rotative speed, rpm |
| n | exponent |
| P | total (stagnation) pressure, $N/cm^2$ abs; psia |
| p | static pressure, $N/cm^2$ abs; psia |
| $R_1,\ldots,R_6$ | inlet to rotor blade row 1,. . ., inlet to rotor blade row 6 |
| Re | blade cord Reynolds number at first stage rotor tip, $\rho_1 V_1' c/\mu_1$ |
| $S_1,\ldots,S_6$ | inlet to stator blade row 1,. . ., inlet to stator blade row 6 |
| T | total (stagnation) temperature, K; $^{o}R$ |
| U | blade speed, m/sec; ft/sec |
| $U/\sqrt{\theta}$ | equivalent blade speed, m/sec; ft/sec |

$V'$ gas velocity relative to rotor tip, m/sec; ft/sec

$W$ weight (mass) flow, kg/sec; lbm/sec

$W\sqrt{\theta}/\delta$ equivalent weight (mass) flow, kg/sec; lbm/sec

$\gamma$ ratio of specific heat at constant pressure to specific heat at constant volume for argon, 1.667

$\delta$ ratio of compressor inlet total pressure to NASA standard sea-level pressure, $P_0/10.1$ N/cm$^2$ abs; $P_0/14.7$ psia

$\eta_{0-8}$ adiabatic efficiency - station 0 to station 8, $T_0\left[(P_8/P_0)^{(\gamma-1)/\gamma} - 1\right]/(T_7 - T_0)$

$\theta$ ratio of compressor inlet total temperature to NASA sea-level temperature, $T_0/288.2$ K; $T_0/518.7^{\circ}$ R

$\mu$ dynamic viscosity, (N)(sec)/m$^2$; lb/(sec)(ft)

$\rho$ density, kg/m$^3$; lb/ft$^3$

Subscripts:

0 station in inlet pipe (25.4 cm or 10 in. upstream of compressor inlet flange)

1 station at rotor 1 inlet

7 station at stator 6 exit, diffuser inlet

8 station in exit pipe (6.4 cm or 2.5 in. downstream of collector exit flange)

## COMPRESSOR DESIGN

A detailed description of the aerodynamic and mechanical design and of the analysis made in arriving at the design values is given in reference 3. A summary of the design is presented herein.

The values of the overall compressor design parameters are presented in table I. Also included in table I are the equivalent design values for standard inlet conditions. The compressor was designed having six stages. It incorporated inlet guide vanes which were designed to impart a swirl in the direction of rotation of 15$^{\circ}$ from the axial direction at the vane tip. This swirl was reduced linearly to zero at the hub. The swirl level and distribution were maintained at the exit of each stator except for stator 6 which turns the flow to the axial direction at all radii. The design tip speed is 246.5 meters per second (811.6 ft/sec) for rotor 1 inlet. The corresponding inlet relative Mach number is 0.788. The hub/tip radius ratio at rotor 1 inlet is 0.69 and increases to 0.73 at stator 6 exit. The hub diameter was held constant through the machine. The throughflow velocity at midpassage was decreased from 123 meters per second (404 ft/sec) at rotor 1 inlet to

93 meters per second (305 ft/sec) at stator 6 exit. Rotor tip diffusion factors varied from 0.42 for rotor 1 to 0.37 for rotor 6. The stator hub diffusion factors varied from 0.44 for stator 1 to 0.39 for stator 4. The stator hub loading then increased to 0.45 for stator 6.

The following design values for each blade row of this compressor are tabulated in reference 3: thermodynamic conditions, gas velocities, actual and effective flow areas, blade loading parameters, Reynolds numbers, incidence angles, deviation angles, and blade geometry parameters.

In arriving at the final compressor design, deviation angles were increased above values arrived at by normal design rules. This increase was based on the data presented in reference 5. The data presented in this reference showed that an increase in deviation angles could be expected at the low Reynolds numbers at which the blading must operate (maximum blade chord Reynolds number of 106 300 at the tip element of rotor 1 to a minimum Reynolds number of 52 200 at the hub element of stator 6). The design deviation angles presented in reference 3 include the increase due to the expected Reynolds number effect.

## APPARATUS AND PROCEDURE

The apparatus and procedure sections of this report are summaries of those presented in reference 4.

### Test Apparatus

The assembled six-stage rotor and inner casing is shown in figure 1. The rotor blades were machined from a titanium alloy (AMS 4928) and are attached to the rotor drum by dovetails and secured by pins. The stator vanes were made of stainless steel and were brazed into semicircular assemblies consisting of an inner and outer shroud ring. The stator inner seal clearances and rotor blade tip clearances (cold) were 0.015 and 0.018 centimeter (0.006 and 0.007 in.), respectively.

Figure 2 is a cross-sectional drawing of the compressor research package. The rotor is supported by two spring-mounted, axially loaded, oil-lubricated ball bearings. Scavenge pressure in the bearing compartments was maintained at a level below argon gas pressure.

The diffuser downstream of the last stator directed the argon gas radially outward into the single outlet collector, which had a constant circular cross section. Figure 3 shows the uninsulated compressor as installed in the test facility. In order to minimize heat transfer during compressor testing, the compressor assembly was insulated with a

high-temperature granular insulating material which was contained by a box built around the compressor. Insulating material was also placed between the compressor support structure and the test stand bedplate. The compressor, fully insulated, is shown in figure 4.

## Test Facility

The test facility used in this investigation is the same as that described in reference 3. Figure 5 is a schematic flow diagram of the test facility.

## Instrumentation

Flow through the compressor was determined from pressure and temperature measurements at a thin-plate orifice installed according to ASME standards in the compressor gas supply line (fig. 5). Compressor performance was based on pressure and temperature measurements at three instrument stations: (1) inlet station located about 25.4 centimeters (10 in.) upstream of inlet flange, (2) stator 6 exit station, and (3) collector exit station located about 7.6 centimeters (3 in.) downstream of exit flange. Combination total pressure/total temperature rakes were employed at the inlet and exit pipe stations. The cross-sectional area at both inlet and collector exit stations was divided into three equal annular areas. Total pressure sensing heads were placed at the arithmetical center of each area. Copper-constantan spike-type thermocouples were placed between the total pressure heads. Three combination total pressure/total temperature rakes were placed $120^{\circ}$ apart at the inlet pipe station, and four combination rakes (equally spaced) were used at the collector exit station. A sample rake is shown in figure 6. Wall static pressure taps of 0.076-centimeter (0.030-in.) diameter were installed at the inlet and exit pipe stations circumferentially midway between rakes.

Instrumentation at the exit of stator 6 consisted of two sets of five individual total pressure probes, two sets of five individual total temperature probes, four outer-wall static pressure taps, and four inner-wall static pressure taps. The probes installed at the stator 6 exit are shown in figure 7. The two sets of total pressure probes were placed circumferentially $180^{\circ}$ apart, as were the two sets of temperature probes. The static pressure taps were placed circumferentially $90^{\circ}$ apart. In this investigation, the total pressure probes were only used in calculating the mass-averaged total temperature. The total temperature probes were semishielded and employed copper-constantan thermocouples. The thermocouple junctions of the two sets of five individual probes were located circumferentially at stator midspacings and radially at 10, 30, 50, 70, and 90 percent of passage height.

In addition to the instrumentation at the three locations described, static pressure wall taps were installed throughout the compressor. Strain-gage-type transducers were employed to measure all pressures. A constant-temperature reference oven (66° C, or 150° F) was used with the research thermocouples in obtaining temperature measurements. Compressor speed was sensed by a magnetic pickup in conjunction with a gear mounted on the compressor shaft. An automatic digital potentiometer was used to record the measurements on paper tape for computor processing of the data. The estimated accuracy of measurement at the highest inlet pressure was as follows: pressure, ±1.5 percent; temperature, ±0.8 K (±1.5° R); and speed, ±0.5 percent. The accuracy of pressure and temperature measurements was lower at the lower inlet pressures.

## Test Procedure

Data were obtained at design speed only. Reynolds number was varied by changing the inlet pressure. At each inlet pressure, the compressor was operated over a range of weight flow from maximum flow to near surge conditions. Surge on this compressor was strong and easily identified even at the lowest inlet pressure. The pressure levels for which the compressor was tested were 1.38, 2.06, 26.6, 4.13, and 6.20 $N/cm^2$ abs (2.0, 3.0, 4.0, 6.0, and 9.0 psia). Throughout the test series, inlet temperature was maintained at nominal design conditions of 298 K (536° R). All data points were taken at time intervals greater than 20 minutes. This was done to establish thermal equilibrium in the compressor. For a detailed discussion and test results of the time required to reach thermal equilibrium, see reference 3.

## Calculation Procedure

Compressor performance was calculated from pressure and temperature measurements taken at the orifice located in the inlet argon supply line, the compressor inlet station, the stator 6 exit station (station 7), and the collector exit station (station 8). Although the total temperature measurements at the exit of the sixth stator and at the collector exit should theoretically agree, it was found that temperatures at stator 6 exit were consistently higher (about 8 to 14 K or 14° to 26° R at design speed). It is felt that this discrepancy is caused by a heat loss from the system and by thermal conduction errors in the exit plane temperature rakes. Because of the heat transfer problems, the collector exit station temperatures $T_8$ were not used. The temperature measured at the sixth stator exit $T_7$ was assumed correct in establishing the temperature rise across the compressor and was used in calculating compressor efficiency. A more complete discussion of the heat transfer problems can be found in reference 4.

Mass-averaged values of pressures and temperatures were used in computing total pressure ratio and efficiency. The design Reynolds number referred to in this report is based on the value at the tip of the first rotor. Reynolds numbers, other than design, were calculated by multiplying the design Reynolds number by the ratio of actual to design inlet pressure. All thermocouple temperatures are corrected for both Mach number and Reynolds number (ref. 6). Equations used in computing compressor performance are defined in the section SYMBOLS.

## RESULTS AND DISCUSSION

The overall performance is shown in figure 8 for the five inlet pressure levels (Reynolds numbers) at which the compressor was tested. The five inlet pressure levels and the corresponding Reynolds numbers are listed in the figure. All data were taken at design equivalent speed of 49 213 rpm and at a nominal design inlet temperature of $536^{\circ}$ R (297.8 K).

As the Reynolds number was decreased from $16.0\times10^4$ to $3.6\times10^4$, both maximum pressure ratio and maximum efficiency show a progressive drop. Maximum pressure ratio decreased from 2.95 to 2.67. Maximum efficiency decreased from 0.765 to 0.677. The flow rate at which maximum efficiency occurred decreased uniformly as the Reynolds number was decreased. The maximum flow rate also decreased with decreasing Reynolds number. However, the surge point seems to be little affected by the change in Reynolds number.

These trends, with the exception of the surge point, can be explained in terms of boundary-layer growth and increasing viscous losses with decreasing Reynolds number. As the boundary layer grows, the effective flow areas are reduced. This causes an increase in throughflow velocities which, in turn, strongly influences the performance characteristics of the compressor. The increased throughflow velocities can, in part, be responsible for the decrease in work input to the gas as the Reynolds number is reduced. The amount of decrease in work is reflected in figure 8(c), where the temperature rise ratio $(T_7 - T_0)/T_0$ is plotted as a function of equivalent weight flow. The sensitivity of the compressor to throughflow velocity is indicated by the decrease in work input with increasing flow for a given inlet pressure (fig. 8(c)).

Another factor that influences work input is a change in deviation angle. As noted in the section COMPRESSOR DESIGN, an adjustment (increase) was made to the design deviation angles in an attempt to account for the effect of the low Reynolds number. Figure 8(c) shows the actual work input to be much higher than design. This very likely is a result of the actual deviation angles being less than design. The other possibility is that the actual boundary-layer blockage was lower than design. If the blockage was low,

it would decrease throughflow velocity, resulting in higher work input. It has been estimated that even if the blockage was zero it would not account for all the increase in measured work input. Thus, it is probable that the actual deviation angles were not as great as the design values.

Changes in throughflow velocity result in changes in incidence angles through the compressor blading. Since incidence angle has a pronounced effect on losses and design incidence angle is normally selected to achieve minimum loss, as incidence angle deviates from design the losses in general will increase. Therefore as the inlet pressure and thus the Reynolds number is changed, the loss will change as a result of both viscous losses directly associated with Reynolds number and changes in incidence angle.

As shown by the dashed line in figure 8(b), the maximum efficiency occurred at progressively lower equivalent weight flows as Reynolds number was reduced. This trend can be explained by the requirement of maintaining an incidence angle (throughflow velocity) close to the minimum blade element loss. In order to maintain a fixed incidence angle as Reynolds number is reduced and losses and blockage increase, the equivalent flow must be reduced.

It was expected that maximum equivalent flow would decrease as the boundary layer thickens with decreasing Reynolds number. This trend was observed, as shown in figure 8. Surge was also expected to occur at progressively lower flows as Reynolds number was reduced. This trend was not observed. Instead, the flow rate at which surge occurred seemed relatively unaffected by Reynolds number. The overall result of this was a decrease in flow range as Reynolds number was reduced. The system is susceptible to surge whenever the slope of the pressure-ratio/flow-rate curve becomes positive. Reynolds number could affect the shape of the pressure-ratio curve by changing stage matching. Within the limitation of the spacing of the data points, examination of the data does not reveal any obvious change in shape of the pressure-ratio characteristic with Reynolds number.

A plot of loss $1 - \eta_{max}$ as a function of percent of design Reynolds number is presented in figure 9 for the maximum efficiency points. This loss is compared to the often-used relation of Reynolds number to loss,

$$\frac{1 - \eta}{1 - \eta_{ref}} = \left(\frac{Re_{ref}}{Re}\right)^n$$

where the subscript ref indicates known values of loss and Reynolds number. For Reynolds numbers above approximately $5 \times 10^4$, the value of the exponent n usually used is 0.2 (ref. 7). A line representing the 0.2 power relation was drawn through the losses at design Reynolds number for comparison to the data. As shown in figure 11, the 0.2 power relation does not accurately predict the losses for the range of Reynolds number

of this investigation. While the average slope of the curve is roughly 0.2, both ends of the curve have significantly different slopes. Below a Reynolds number of $5\times10^4$, or approximately 50 percent of design Reynolds number for this compressor, single-stage compressor losses have been shown to vary with the 0.5 power (ref. 8). This is analogous to the drag coefficient on a smooth flat plate. For very low Reynolds numbers, where the flow is laminar, the drag coefficient is inversely proportional to the 0.5 power of Reynolds number. Although this would tend to explain the lower Reynolds number data, the laminar boundary layer, which should accompany this, seems unlikely, particularly in a multistage compressor. The high degree of unsteady flows in a multistage compressor should promote turbulence and, thus, hasten transition. Another, and more likely, explanation is that a mismatch between stages is beginning to occur. In a well-matched compressor, each stage will be at or near its peak efficiency at design flow rate. Stage mismatching occurs when one or more stages are not operating at their peak efficiency point. The changes in incidence and deviation angles caused by Reynolds number could result in a mismatch between stages.

The loss approaches a constant value at the higher Reynolds numbers, as shown in figure 9. Here again a growing stage mismatch might be responsible for the deviation from the 0.2 power. Another possibility is that the blade surfaces are approaching the aerodynamically rough condition (i.e., the minimum boundary-layer thickness is controlled by surface roughness).

The 0.2 and 0.5 power relations can only be expected to predict the loss variation with Reynolds number where the only variable components of the total loss are viscous losses. Correlating the maximum efficiency points, instead of the efficiency at a given flow, tends to isolate the viscous losses. Even though maximum efficiency points are used, such losses as tip clearance losses, secondary flow losses, separation losses, and losses related to incidence angle can also vary as a function of Reynolds number. Therefore, an accurate determination or prediction of Reynolds number effect requires the ability to better isolate the viscous losses.

Wall static pressure distribution through the compressor operating at design speed is presented in figure 10 for three Reynolds numbers. The design static pressure distribution is also shown in figure 10. Some of the pressures are missing due to transducer failure. A uniform rise in static pressure was observed for all inlet pressures. This tends to indicate that there are no blade rows operating in a severe off-design condition. The large differences between the pressure distributions (fig. 10) is consistent with the previously noted large changes in work input (fig. 8(c)) over the range of Reynolds numbers investigated. It is interesting to note that the design pressure distribution coincides almost exactly with the distribution for the lowest Reynolds number. This again illustrates the large increase in pressure ratio obtained in this machine over the design values.

The variation of loss with Reynolds number for a 15.2-centimeter (6-in.) centrifugal compressor designed for the same overall conditions as the axial compressor is presented in reference 2. A comparison of the variation of loss with percent design inlet pressure (percent design Reynolds number) for the two compressors is shown in figure 11. The performance obtained from the centrifugal compressor shows it to be less sensitive to inlet pressure than the axial compressor in the lower inlet pressure range. At the higher inlet pressure, both compressors show a leveling off of loss. Unpublished data obtained from a 16.4-centimeter (6.44-in.) diameter sweptback bladed centrifugal compressor also designed for the same overall condition show it also to be less sensitive to inlet pressure than the axial compressor. In fact, the 16.4-centimeter machine was even less sensitive to inlet pressure than the 15.2-centimeter machine. The Reynolds number performance of a scale version of the 16.4-centimeter-diameter compressor is reported in reference 9 and also shows the lower sensitivity to Reynolds number in the range of Reynolds number tested.

The sensitivity of any compressor, axial or centrifugal, to inlet pressure in part depends on the flow regime where it operates. If the compressor is operating in the flow regime where the surfaces are considered aerodynamically rough, loss is not a function of Reynolds number, as discussed earlier in this report. When it is operating in the flow regime where the surfaces are considered aerodynamically smooth, the viscous portion of the losses will vary with Reynolds number. An additional factor which can affect the sensitivity of a compressor to inlet pressure is the design flow match between blade rows relative to the flow match which would result in minimum loss. One might expect the axial compressor to be more sensitive than the centrifugal compressor to changes in inlet pressure since it has more blade rows to become mismatched. It would appear that, with the present level of design knowledge for low-Reynolds-number machines, a larger reduction in performance with inlet pressure can be expected for the multistage axial compressor than for the comparable centrifugal compressor.

## SUMMARY OF RESULTS

A 9.4-centimeter (3.7-in.) diameter six-stage axial-flow compressor was tested in argon to establish the effect of Reynolds number on the overall performance. The compressor was run at design speed for five different inlet pressures from 1.38 to 6.2 $N/cm^2$ abs (2.0 to 9.0 psia). This change in inlet pressure corresponds to a range of Reynolds number from $3.6\times10^4$ to $16.0\times10^4$. The following changes in performance were noted for this range of Reynolds number:

1. As the Reynolds number decreased, the maximum efficiency dropped from 0.765 to 0.677.

2. The maximum total pressure ratio dropped from 2.95 to 2.67 as the Reynolds number was decreased.

3. The work input, as shown by the temperature rise ratio across the machine, also decreased with decreasing Reynolds number. In addition, the work input was much higher than the design value.

4. The maximum flow rate decreased with decreasing Reynolds number, while the flow rate at which surge occurred remained relatively unchanged.

5. Maximum efficiency occurred at progressively lower weight flows as Reynolds number was reduced.

6. Significant deviation was noted from the 0.2 power relation often used to express the variation of loss with Reynolds number. This deviation occurred at both ends of the Reynolds number range investigated, while the mid-region was in close agreement with the 0.2 power relation.

7. A comparison of the losses for this axial compressor with those of a centrifugal compressor designed for the same overall conditions showed the centrifugal compressor to be less sensitive to inlet pressure in the lower inlet pressure level tested. At the higher inlet pressures, both compressors showed a leveling off of the losses.

Lewis Research Center,
National Aeronautics and Space Administration,
Cleveland, Ohio, November 19, 1971,
764-74.

## REFERENCES

1. Tysl, Edward R.; Ball, Calvin L.; Weigel, Carl; and Heidelberg, Laurence J.: Overall Performance in Argon of a 6-Inch Radial-Bladed Centrifugal Compressor. NASA TM X-1622, 1968.

2. Heidelberg, Laurence J.; Ball, Calvin L.; and Weigel, Carl: Effect of Reynolds Number on Overall Performance of a 6-Inch Radial Bladed Centrifugal Compressor. NASA TN D-5761, 1970.

3. Cohen, R.; Gilroy, W. K.; and Marchant, R. D.: Compressor Research Package for Research and Development of High Performance Axial-Flow Turbomachinery. Rep. PWA-2933, Pratt & Whitney Aircraft (NASA CR-54884), Mar. 1967.

4. Tysl, Edward R.; Heidelberg, Laurence J.; and Weigel, Carl: Overall Performance in Argon of a 3.7-Inch Six-Stage Axial-Flow Compressor. NASA TM X-2194, 1971.

5. Rhoden, H. G.: Effect of Reynolds Number on the Flow of Air Through a Cascade of Compressor Blades. Rep. R & M 2919, Ministry of Supply, Aeronautical Research Council, 1956.

6. Glawe, George E.; Simmons, Frederick S.; and Stickney, Truman M.: Radiation and Recovery Corrections and Time Constants of Several Chromel-Alumel Thermocouple Probes in High-Temperature, High-Velocity Gas Streams. NACA TN 3766, 1956.

7. Bullock, R. O.: Analysis of Reynolds Number and Scale Effects on Performance of Turbomachinery. J. Eng. Power, vol. 86, no. 3, July 1964, pp. 247-256.

8. Carter, A. D. S.; Moss, C. E.; Green, G. R.; and Annear, G. G.: The Effect of Reynolds Number on the Performance of a Single Stage Compressor. Rep. R. 204, National Gas Turbine Establishment, Gt. Britain, May 1957.

9. Weigel, Carl; and Ball, Calvin L.: Reynolds Number Effect On Overall Performance of a 10.8-Centimeter (4.25-in.) Sweptback-Bladed Centrifugal Compressor. NASA TN D-6640, 1972.

TABLE I. - COMPRESSOR DESIGN PARAMETERS

[Working fluid, argon.]

| Compressor design parameters | Based on design inlet pressure and temperature | Based on standard inlet pressure and temperature |
|---|---|---|
| Compressor inlet total pressure, $P_0$, $N/cm^2$ abs (psia) | 4.1 (6) | 10.1 (14.7) |
| Compressor inlet total temperature, $T_0$, K ($^oR$) | 298 (536) | 288.2 (518.7) |
| Weight (mass) flow rate, W, kg/sec (lbm/sec) | 0.278 (0.611) | 0.69 (1.52) |
| Compressor total pressure ratio, $P_7/P_0$ | 2.365 | [a]2.365 |
| Compressor total pressure ratio, $P_8/P_0$ | 2.3 | [a]2.3 |
| Compressor adiabatic efficiency, $\eta_{0-7}$ | 0.858 | [a]0.858 |
| Compressor adiabatic efficiency, $\eta_{0-8}$ | 0.825 | [a]0.825 |
| Compressor total temperature ratio, $T_7/T_0 = T_8/T_0$ | 1.494 | [a]1.494 |
| Compressor rotational speed, N, rpm | 50 000 | 49 183 |

[a]Approximate equivalent values which may differ from design values as a result of differences in Reynolds numbers between design and standard inlet conditions.

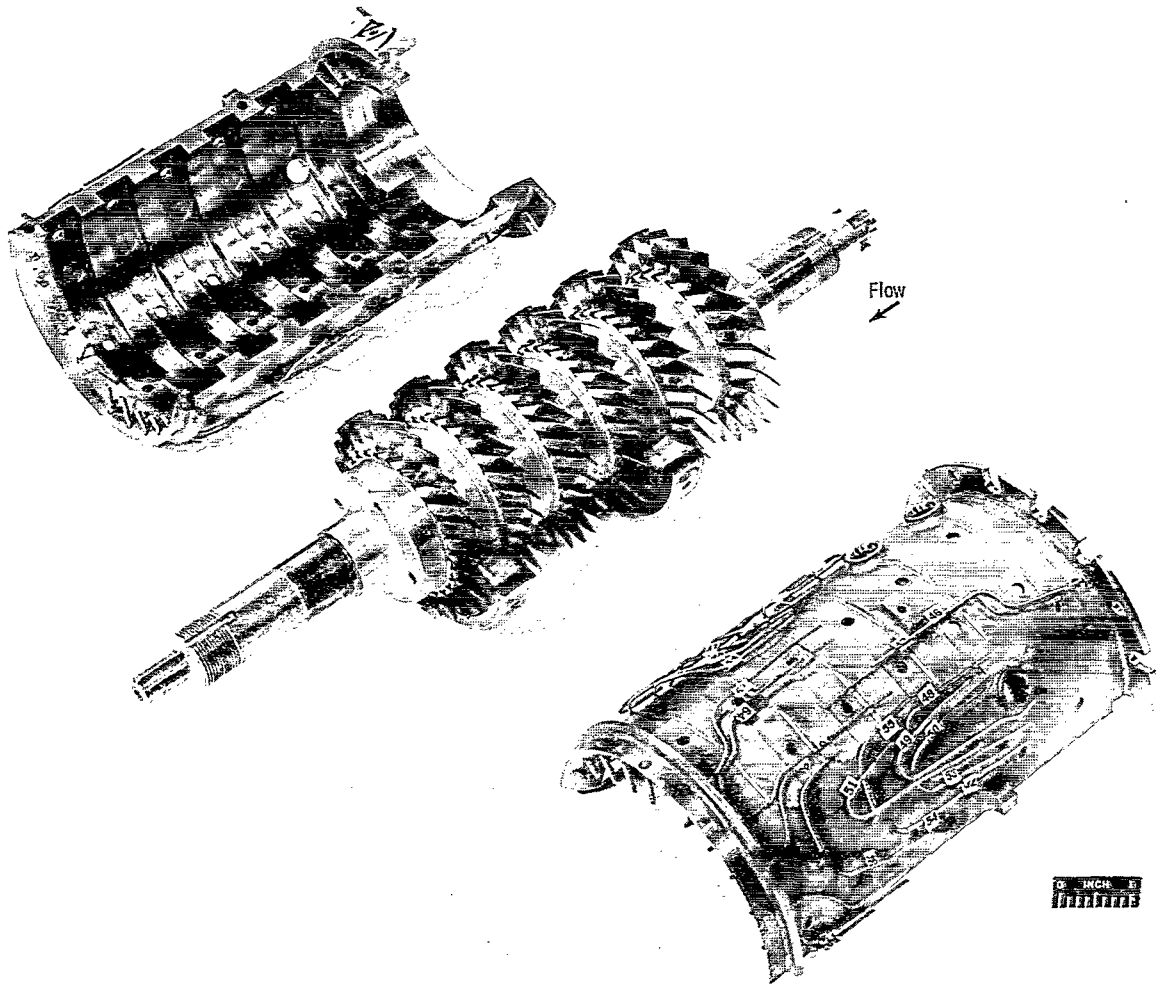


C-66-4625

Figure 1. - Six-stage rotor and split casing.

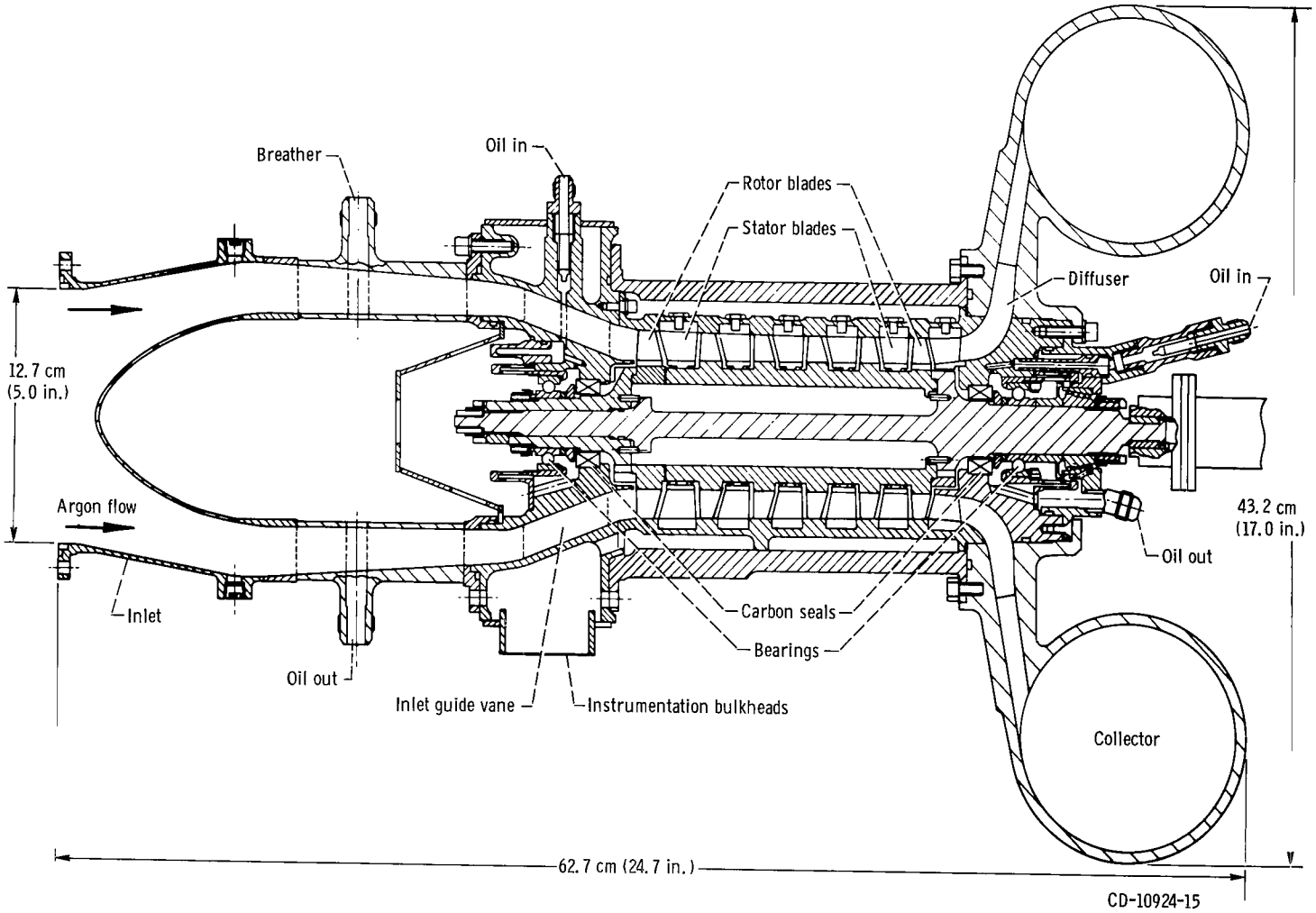


Figure 2. - Cross section of research compressor.

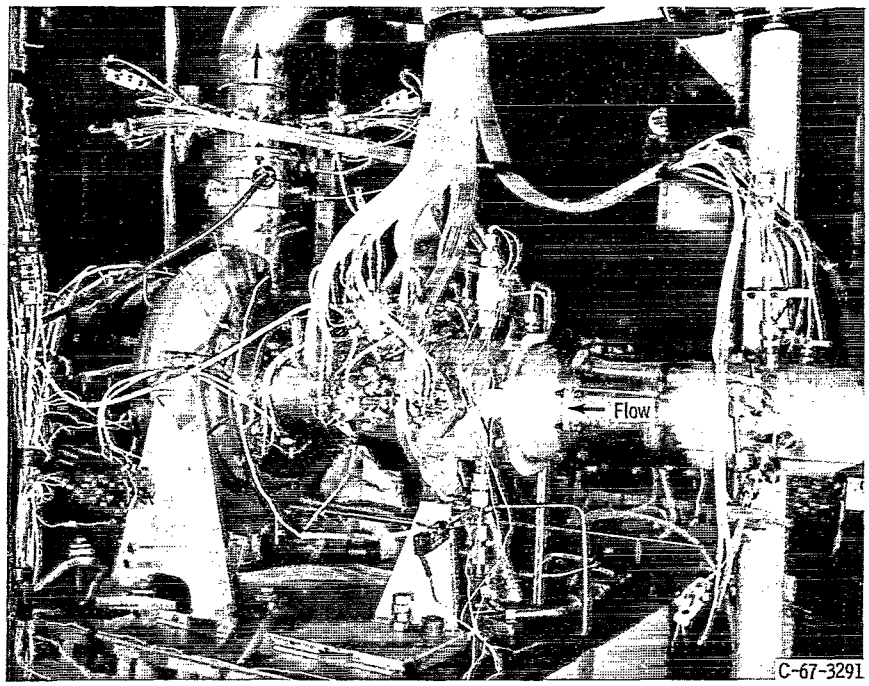


Figure 3. - Uninsulated compressor.

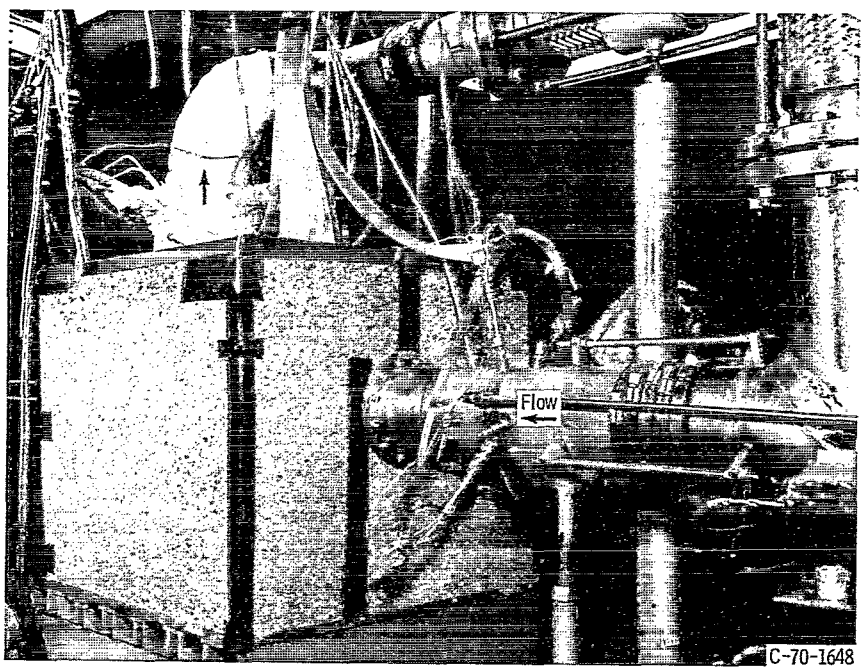


Figure 4. - Compressor fully enclosed in insulation.

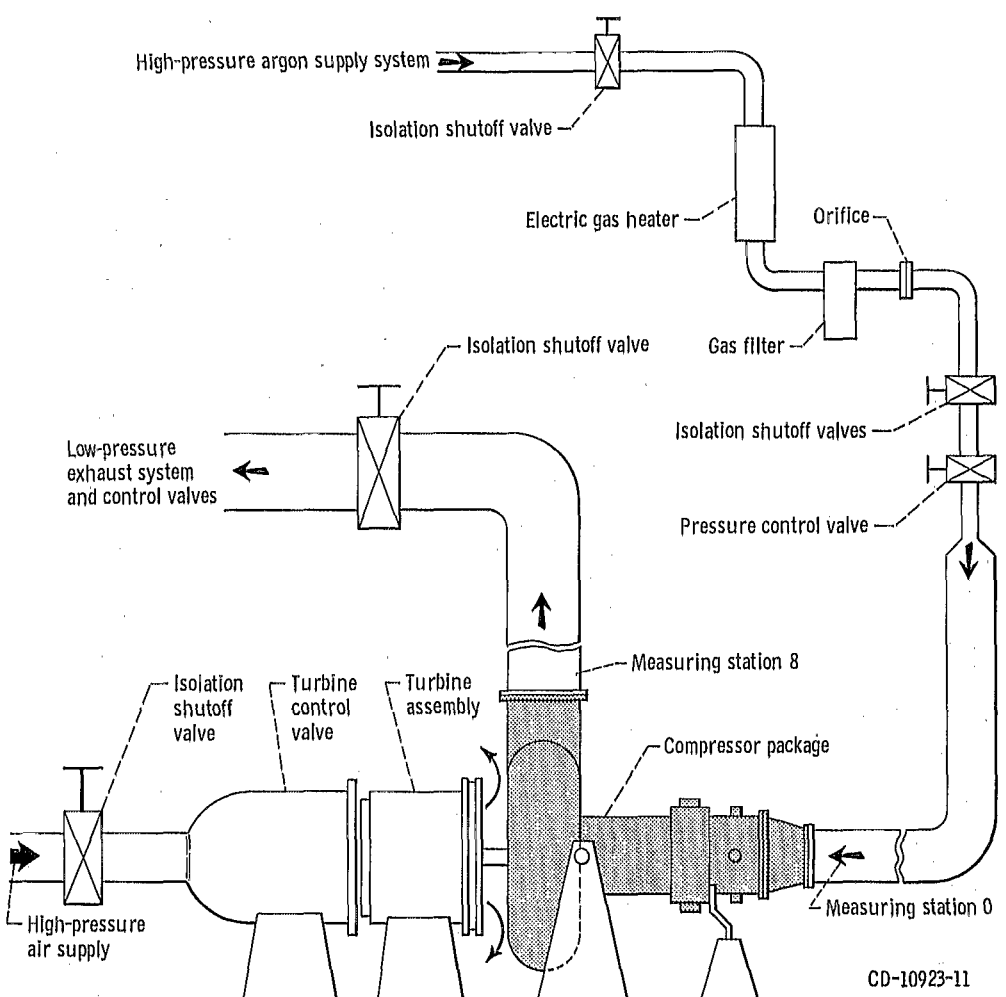


Figure 5. - Flow diagram of compressor test facility.

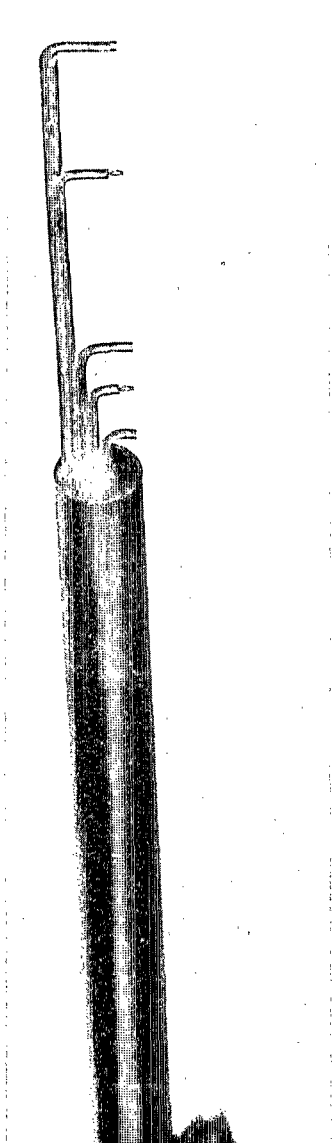


Figure 6. - Combination total pressure and total temperature rake.

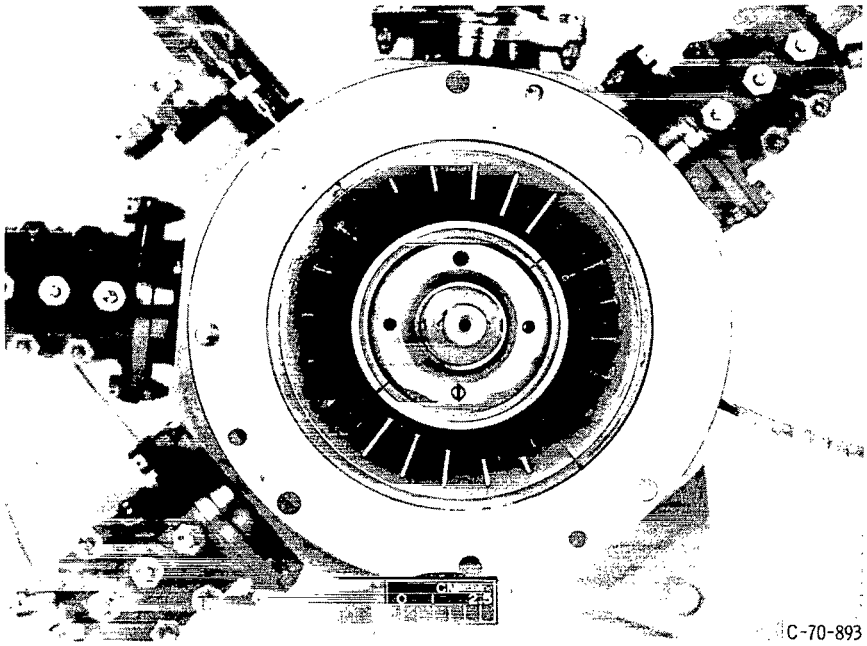

C-70-893

Figure 7. - Total pressure and total temperature probes at stator 6 exit.

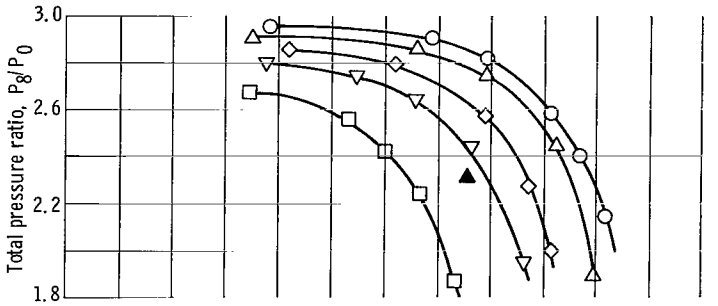


| Inlet pressure, $N/cm^2$ abs | (psia) | Compressor Reynolds number |
|---|---|---|
| ○ 6.20 | (9.0) | $16.0 \times 10^4$ |
| △ 4.13 | (6.0) | 10.6 |
| ◇ 2.66 | (4.0) | 7.2 |
| ▽ 2.06 | (3.0) | 5.3 |
| □ 1.38 | (2.0) | 3.6 |
| ▲ Design point | | |

(a) Total pressure ratio at design speed.

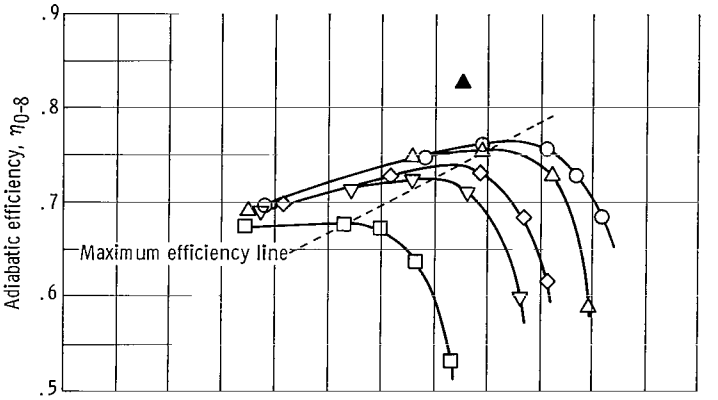


(b) Efficiency at design speed.

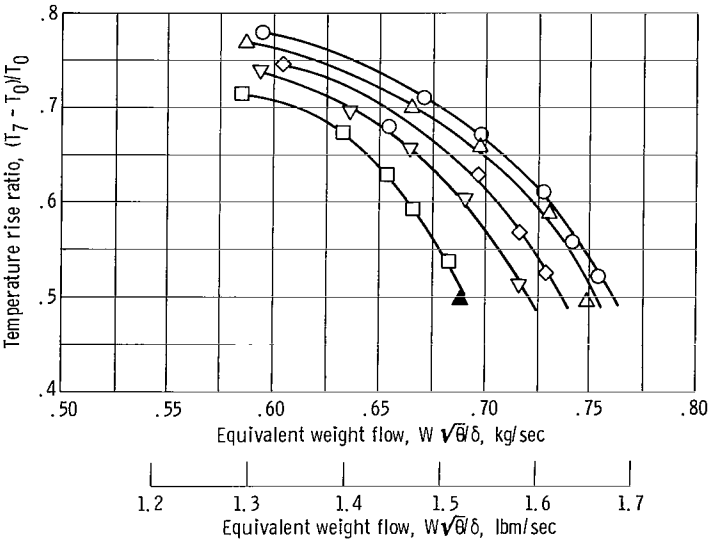


(c) Temperature rise ratioed to inlet temperature at design speed.

Figure 8. - Overall performance of a 9.4-centimeter (3.7-in.) diameter six-stage axial-flow compressor.

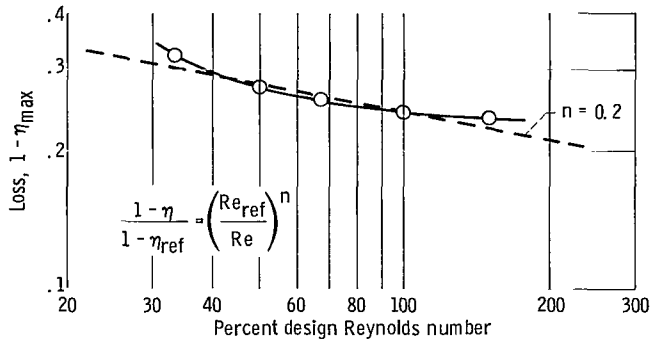


Figure 9. - Loss for 9.4-centimeter (3.7-in.) six-stage axial-flow compressor at design speed. Design Reynolds number, 106 300.

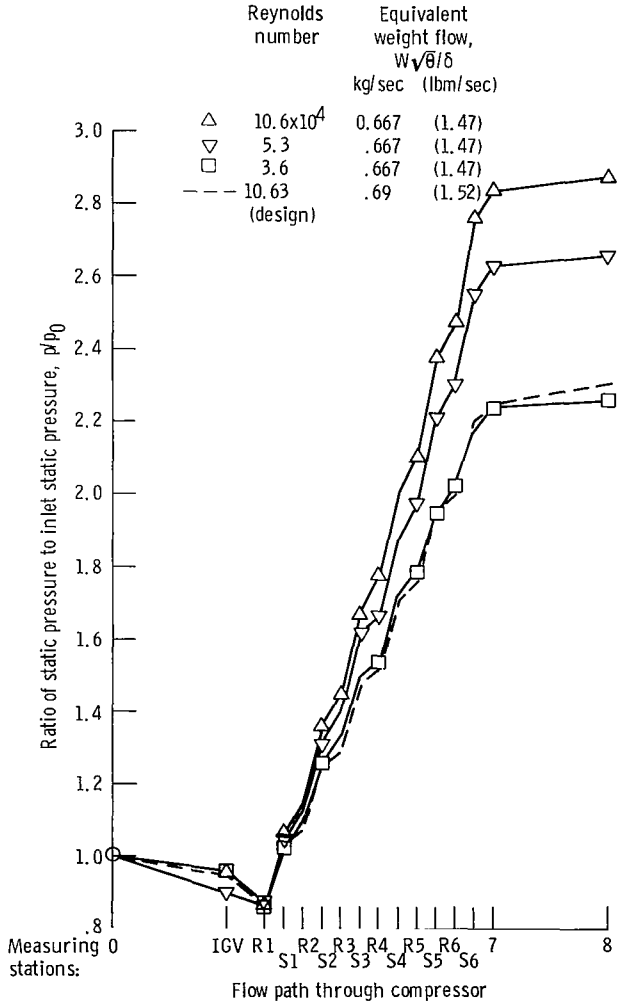


Figure 10. - Wall static pressure distribution at design speed. (See SYMBOLS for explanation of measuring stations.)

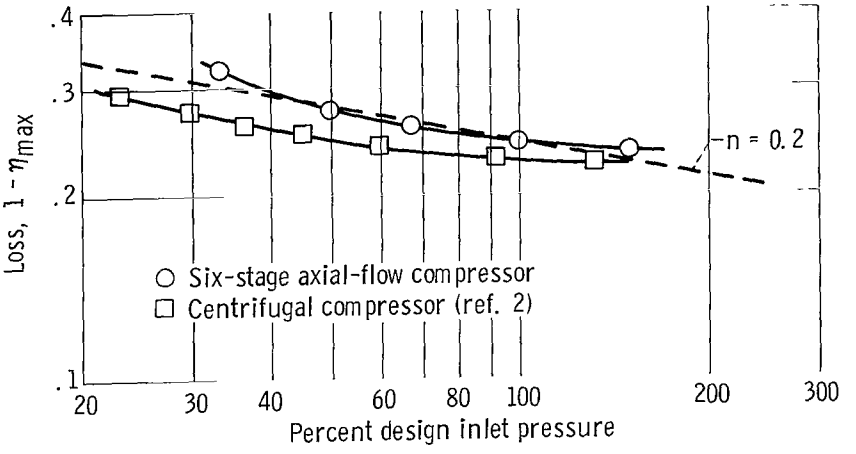


Figure 11. - Loss as function of percent design inlet pressure at design speed.



NASA-Langley, 1972 —— 1

NATIONAL AERONAUTICS AND SPACE ADMISTRATION
WASHINGTON, D.C. 20546

OFFICIAL BUSINESS
PENALTY FOR PRIVATE USE $300

FIRST CLASS MAIL

POSTAGE AND FEES PAID
NATIONAL AERONAUTICS AND
SPACE ADMINISTRATION

U.S.MAIL

018 001 C1 U 01 720128 S00903DS
DEPT OF THE AIR FORCE
AF WEAPONS LAB (AFSC)
TECH LIBRARY/WLOL/
ATTN: E LOU BOWMAN, CHIEF
KIRTLAND AFB NM 87117

POSTMASTER: If Undeliverable (Section 158 Postal Manual) Do Not Return

*"The aeronautical and space activities of the United States shall be conducted so as to contribute . . . to the expansion of human knowledge of phenomena in the atmosphere and space. The Administration shall provide for the widest practicable and appropriate dissemination of information concerning its activities and the results thereof."*

—NATIONAL AERONAUTICS AND SPACE ACT OF 1958

# NASA SCIENTIFIC AND TECHNICAL PUBLICATIONS

TECHNICAL REPORTS: Scientific and technical information considered important, complete, and a lasting contribution to existing knowledge.

TECHNICAL NOTES: Information less broad in scope but nevertheless of importance as a contribution to existing knowledge.

TECHNICAL MEMORANDUMS: Information receiving limited distribution because of preliminary data, security classification, or other reasons.

CONTRACTOR REPORTS: Scientific and technical information generated under a NASA contract or grant and considered an important contribution to existing knowledge.

TECHNICAL TRANSLATIONS: Information published in a foreign language considered to merit NASA distribution in English.

SPECIAL PUBLICATIONS: Information derived from or of value to NASA activities. Publications include conference proceedings, monographs, data compilations, handbooks, sourcebooks, and special bibliographies.

TECHNOLOGY UTILIZATION PUBLICATIONS: Information on technology used by NASA that may be of particular interest in commercial and other non-aerospace applications. Publications include Tech Briefs, Technology Utilization Reports and Technology Surveys.

*Details on the availability of these publications may be obtained from:*

**SCIENTIFIC AND TECHNICAL INFORMATION OFFICE**

**NATIONAL AERONAUTICS AND SPACE ADMINISTRATION**

**Washington, D.C. 20546**